Physiological and metabolic responses of freshwater and brackish strains of Microcystis aeruginosa acclimated to a salinity gradient: insight into salt tolerance

Maxime Georges Des Aulnois, Pauline Roux, Amandine Caruana, Damien Réveillon, Enora Briand, Fabienne Herve, Véronique Savar, Myriam Bormans, Zouher Amzil

Physiological and metabolic responses of freshwater and brackish strains of *Microcystis aeruginosa* acclimated to a salinity gradient: insight into salt tolerance

Maxime Georges des Aulnois,[a]# Pauline Roux,[a] Amandine Caruana,[a] Damien Réveillon,[a] Enora Briand,[a] Fabienne Hervé,[a] Véronique Savar,[a] Myriam Bormans[b] Zouher Amzil[a]

[a]Phycotoxins Laboratory, IFREMER, Nantes, France

[b]Univ Rennes, CNRS, ECOBIO - UMR 6553, F-35000 Rennes, France

Running Head: Physiology of salt tolerance in *M. aeruginosa*

maxime.desaulnois@gmail.com

Abstract

Proliferation of microcystin (MC) producing *Microcystis aeruginosa* in brackish waters has been described in several locations and represents a new concern for public and environmental health. While the impact of a sudden salinity increase on *M. aeruginosa* physiology has been studied, less is known about the mechanisms involved in salt tolerance after acclimation. This study aims to compare the physiological responses of two strains of *M. aeruginosa* (PCC 7820 and PCC 7806), isolated from contrasted environments, to increasing salinities. After acclimation, growth, MC production and metabolomic analyses were conducted. For both strains, salinity decreased the biovolume, the growth and MC production rates and induced the accumulation of polyunsaturated lipids identified as monogalactosyldiacylglycerol. The distinct salt tolerance (7.5 and 16.9) obtained between the freshwater (PCC 7820) and the brackish water (PCC 7806) strains suggested different strategies to cope with the osmotic pressure, as revealed by targeted and untargeted metabolomic analyses. Accumulation of trehalose as the main compatible solute was obtained in the freshwater strain while sucrose was mainly accumulated in the brackish one. Moreover, distinct levels of glycine betaine and proline accumulation were noted. Altogether, metabolomic analysis illustrated a strain-specific response to salt tolerance, involving compatible solutes production.

Importance

Blooms of *Microcystis aeruginosa* and production of microcystins is one of the major issue in eutrophic freshwater bodies. Recently, an increasing number of proliferations of *M. aeruginosa* in brackish water has been documented. Occurrence of both *M. aeruginosa* and microcystins in coastal areas represents a new threat for human and environmental health. In order to better describe the mechanisms involved in *Microcystis* proliferation in brackish water, this study used two *M. aeruginosa* strains isolated from fresh and brackish waters. High salinity reduced the growth rate and microcystin production rate of *M. aeruginosa*. In order to cope with higher salinities, the strains accumulated different cyanobacterial compatible solutes, as well as unsaturated lipids, explaining their distinct salt tolerance.

Introduction

Due to anthropogenic activities and climate change, many freshwater ecosystems are expected to experience an increase in salinity (S) (1). This phenomenon, exacerbated by drought, hydrologic alterations, land use and sea level rise (2–5), is predicted to favor the development and expansion of freshwater cyanobacteria versus other freshwater phytoplankton (6, 7). As many freshwater cyanobacteria produce a variety of toxins affecting both animal and human health (8), this expansion is particularly problematic, especially concerning the genus *Microcystis*. Indeed, *Microcystis* is currently recognized as one of the most pervasive toxic cyanobacteria in freshwater ecosystems as blooms have been reported on all continents but Antarctica (9). This global occurrence is explained by both a high genomic and phenotypic plasticity (9, 10). Therefore, the biotic and abiotic factors influencing blooms of toxic *Microcystis* have been well-studied in freshwater ecosystems (9). However, the influence of salinity on their development was overlooked despite the observation of *Microcystis* and the hepatotoxic microcystins (MC) in many coastal areas (11). In most reported studies, the records of *Microcystis* in coastal areas were due to the transfer of a *Microcystis* bloom across the freshwater-to-marine continuum (12–17). This transfer to high salinity conditions resulted in cell lysis and the release of soluble MCs in the water (17–19). Such occurrences of *Microcystis* in coastal areas resulted ultimately in MC accumulation in marine organisms and represented a potential new food-borne route exposure to human health. As a result, most experimental studies conducted on the impact of salinity on *Microcystis* focused on salt stress experiments (19–24), especially on *Microcystis aeruginosa* as the main bloom-forming species among this genus. Those studies defined *M. aeruginosa* salinity tolerance between freshwater ecosystems to

100 the upper limit of the oligohaline areas (5 < S < 18) (20–22, 24–27). However, salt
101 stress experiments did not allow to determine the potential of *Microcystis* to form
102 blooms in brackish waters. Less frequently, blooms of *Microcystis* have also been
103 reported in brackish waters (11, 28). The first experimental study on the physiology of
104 *M. aeruginosa* PCC 7806 acclimated to distinct salinities (0 to 17.5) was conducted
105 by Tonk et al. (2007). This study concluded that growth and MC cellular quota of *M.*
106 *aeruginosa* decreased above a salinity of 10. Whereas, after acclimation of isolated
107 strains of *M. aeruginosa*, Mazur Marzec et al. (2010) did not find any effect of *salinity*
108 (0 to 14) on the total biomass of acclimated *M. aeruginosa* isolates after 3 weeks of
109 culture in controlled conditions but they also observed a decrease in MC cellular
110 quotas above salinity 7.
111 Salinity tolerance of cyanobacteria is mainly conditioned by the ability of cells to
112 regulate their internal osmosis through the regulation of the intracellular ionic balance
113 and the accumulation of compatible solutes (31). So far, several compounds were
114 clearly identified as compatible solutes in cyanobacteria which are sucrose,
115 trehalose, glucosylglycerol, glucosylglycerate, glycine betaine (GB), glutamate
116 betaine and proline (31). In addition, dimethylsulfoniopropionate (DMSP) has been
117 described as a putative compatible solute in certain microalgae (32, 33). DMSP or its
118 by-product DMS were more rarely detected in cyanobacteria. As far as we know,
119 DMSP was reported in the marine species *Microcoleus lyngbyaceus* and *M.*
120 *chtonoplastes*, *Lyngbya aestuari, Trichodesmium erythraeum*, the brackish water
121 genus *Synechocystis* sp. and the freshwater species *Aphanizomenon flos-aquae*
122 (33–35). In the genus *Microcystis*, the glucosylglycerol was the first identified
123 compatible solute in *M. firma* (36). Concerning *M. aeruginosa* PCC 7806 strain
124 specifically, Kolman et al. (37) identified the compatible solute sucrose as the main

metabolite explaining its salt tolerance and Sandrini et al. (38) showed that this strain and its non MC-producing mutant were less sensitive to cationic stress than other freshwater isolates. The strain *M. aeruginosa* PCC 7806 was indeed isolated in brackish water and possesses genes involved in osmotic stress response which are not present in the other freshwater isolates (37, 38). Recently, Tanabe et al. (2018) confirmed that the salt tolerance of *Microcystis* strains isolated from brackish water may be attributable to the presence of sucrose genes that were absent in freshwater isolates. Altogether, those studies led us to hypothesize that discrepancies in salinity tolerance between strains isolated from freshwater and brackish water could be explained by distinct physiological mechanisms involving the synthesis of compatible solutes. Based on acclimated strains to different salinities, this study used a quantitative analysis of MCs and potential compatible solutes and a non-targeted metabolomic approach to provide new insights about the potential mechanisms involved in salt tolerance to better understand the occurrence of *M. aeruginosa* in brackish waters.

Results

Growth and salinity tolerance at contrasted salinities

After acclimation, *M. aeruginosa* PCC 7820 displayed positive growth at salinities between 0.6 and 7.5 while *M. aeruginosa* PCC 7806 grew over a wider range of salinities up to 16.9. Only at the lowest salinity (S = 0.6), the growth of both strains reached a stationary phase after an exponential growth phase (4-28 days for PCC 7820; 4-24 days for PCC 7806; Fig. 1A and B). During the exponential growth phase at salinity control, the cell concentration increased from 3.9×10^6 cells mL^{-1} ($\pm 3.5 \times 10^4$) to 5.8×10^7 cells mL^{-1} ($\pm 1.3 \times 10^6$) for PCC 7820 and 2.2×10^6 cells mL^{-1} ($\pm$

9.7 x 10^4) to 4.7 x 10^7 cells mL^{-1} (± 4.1 x 10^6) for PCC 7820. Compared to the control, cell concentration of both strains increased more slowly with higher salinities (Fig. 1A and B). Indeed, the growth rates of *M. aeruginosa* PCC 7820 and PCC 7806 (Fig. 2) differed significantly with increasing salinities (ANOVA, PCC 7820: *P* value < 1.5 x 10^{-5}; PCC 7806: *P* value < 6.6 x 10^{-11}). For the strain *M. aeruginosa* PCC 7820, no statistical difference was observed between control salinity at 0.6 and 3.7, but a significant decrease with control was obtained at 6.4 and 7.5. Between S = 0.6 (μ = 0.37 ± 0.03 day^{-1}) and S = 7.5 (μ = 0.16 ± 0.03 day^{-1}), the growth rate of this strain differed by 2.3. No significant statistical difference was observed between growth rates of *M. aeruginosa* PCC 7806 up to 8.4. At S = 10.7 and at higher salinities, the growth rate of *M. aeruginosa* was significantly lower compared to the control (Dunnett's test, *P* values < 0.05). The growth rate of *M. aeruginosa* PCC 7806 differed by 2.6 between the control condition (μ = 0.42 ± 0.02 day^{-1}) and the highest salinity 16.9 (μ = 0.16 ± 0.02 day^{-1}) (Fig. 2).

Although salinity affected the growth rate of both strains, it did not affect the maximum quantum yield of the photosystem II. The F_v/F_m values recorded from cultures of *M. aeruginosa* PCC 7820 remained in a restricted range between 0.43 and 0.55 for all salinity conditions and sampling times. The values for *M. aeruginosa* PCC 7806 were also stable at each salinity between 0.29 and 0.59 (see Fig. S1 in the supplemental material). Lowest values of F_v/F_m were recorded for both strains at the lowest salinity (S = 0.6).

A comparison of the relative cell size at day 14 expressed as FSC intensity was conducted. For the strain PCC 7820, the FSC value at salinity control was 6.1 x 10^5 ± 0.2 x 10^5 and 4.8 x 10^5 ± 0.1 x 10^5 at the highest salinity 7.5. Similarly, for the strain PCC 7806, the FSC value at salinity control was 8.3 x 10^5 ± 0.4 x 10^5 and 3.7

175 x 10^5 ± 0.04 x 10^5 at the highest salinity 16.9. Relative cell size on day 14 at each
176 salinity significantly decreased compared to control for both strains with smaller
177 cells at higher salinities (ANOVA; Dunnett's test; *P* value < 0.05; see Fig. S2 in the
178 supplemental material).
179
180 **Toxin profiles and toxin production of *Microcystis aeruginosa***
181 Five different MC variants were quantified in *M. aeruginosa* PCC 7820 (MC-LR, MC-
182 LY, MC-LW, MC-LF and dmMC-LR; Fig. 3A) and two variants in PCC 7806 (MC-LR
183 and dmMC-LR; Fig. 3B). Cellular quotas for each MC variant of *M. aeruginosa* PCC
184 7820 increased during the exponential growth at low and intermediate salinities (S =
185 0.6-6.4), whereas, this pattern was not observed at the highest salinity (S = 7.5)
186 where MC quotas decreased over time (Fig. 3A). The MC-LR and dmMC-LR cellular
187 quotas of *M. aeruginosa* PCC 7806 remained globally constant during the entire
188 monitoring period at all salinities except at the highest one (S = 16.9). On average for
189 all sampling days at S =16.9, the MC-LR and dmMC-LR quotas differed by 2.3 and
190 2.5 respectively compared to the control (Fig. 3B). For both strains, MC cellular
191 quotas were significantly affected by salinity, time and their interaction (two-way
192 ANOVAs: *P* value < 0.05). Proportion of each variant in total MCs for PCC 7820
193 changed between 1.3 and 2.7-fold over time and salinity. The same range was
194 obtained in PCC 7806 where MC-LR and dmMC-LR proportions changed by 1.2 and
195 2.5-fold (data not shown).
196 Extracellular MCs for *M. aeruginosa* PCC 7820 cultures on day 4 represented 11% (
197 ± 1.3%) of the total MC quantified for the control salinity but increased sharply with
198 salinity (44, 48 and 65% at salinity 3.6, 6.4 and 7.5) (Fig. 4A). For all salinities, but
199 7.5, the proportion of total extracellular MC variants decreased with time and the

accumulation of biomass. At salinities 0.6, 3.6 and 6.4, this proportion was reduced respectively to 1.6% (± 0.3%), 3.1% (± 1.1%) and 11% (± 1.7%) by day 24. However at salinity 7.5, an increase in the proportion of extracellular MC variants occurred between days 14 and 24, from 42% (± 3.1%) to 86% (± 2.3%) (Fig. 4A). For *M. aeruginosa* PCC 7806, the proportion of MC retrieved in the culture medium was maximum 4 days after the inoculation between 16% (± 2.7%) and 68% (± 2.3%). This proportion decreased over time at all salinities (Fig. 4B).

The net production rate of total MCs in both strains decreased significantly at higher salinities (PCC 7820: ANOVA One-Way: $p = 5.41 \times 10^{-8}$, PCC 7806: Kruskall-Wallis test $p = 0.046$, data not shown). For both strains and salinities, growth rate and net MC production rate were linearly correlated according to Pearson correlation test (PCC 7820 *P* value = 8.8×10^{-4}, PCC 7806 *P* value = 1.1×10^{-8}).

DMSP, GB and proline cellular concentrations

In all of the samples, the quantity of DMSP was below the detection limit (50 nM). When detected, GB and proline were quantified in both strains of *M. aeruginosa* (Fig. 5). In *M. aeruginosa* PCC 7820, GB cellular concentration increased with the salinity but decreased over time (Fig. 5A). At each sampling time, GB cellular quotas were higher at S = 7.5 compared to the control concentrations ranging from 1.2×10^{-3} to 4.4×10^{-3} fmol cell^{-1} and 2.0×10^{-4} to 2.4×10^{-3} fmol cell^{-1} respectively (Fig. 5A). Similar results were obtained for PCC 7806 but with lower GB concentrations (Fig. 5B). At the salinity control and 3.6, the cellular quota of GB was below the detection limit (50 nM) while GB was quantified at salinities between 10.7 and 16.9 (Fig. 5B). On average over the salinities and sampling times, the cellular quota of proline in *M. aeruginosa* PCC 7820 was three times greater than for the strain *M. aeruginosa* PCC

7806 (Fig. 5A and B). For both strains, cellular quotas of proline increased with salinity, but this pattern appeared to be more intense in *M. aeruginosa* PCC 7820 (Fig. 5A).

Metabolomic analyses

Metabolomic analyses were performed to evaluate the impact of an increase in salinity on the metabolomes of *M. aeruginosa* PCC 7820 and PCC 7806 and to highlight putative biomarkers of salinity acclimation for both strains. Based on a matrix of 83 compounds after data filtrations, the resulting PCA score plot was represented in Fig. 6 and the total variance due to the two main axes accounted for 81.3%. The first principal component represented the distinction between the two strains and illustrated the intraspecific variability of *M. aeruginosa* (59.3%) while the second (22%) allowed for a clustering depending on salinity (Fig. 6). Hence, for each strain, after acclimation period, the salinity of the medium induced an evolution of the metabolome of the two *M. aeruginosa* strains. For each strain, two groups of salinity were noted. For *M. aeruginosa* PCC 7806, only the highest salinity (i.e. S =16.9) formed a distinct cluster, while the two lowest and the two highest salinities were separately grouped for *M. aeruginosa* PCC 7820.

In order to pinpoint metabolites that were differently expressed, we used PLS-DA that is a well-known dimension reduction method for biomarker discovery in metabolomics (39, 40). It constructs a set of orthogonal components that maximize the sample covariance between the response and the linear combination of the predictor variables, thus focusing on class separation (41). Using a PLS-DA and VIP scores, it was possible to highlight 35 and 31 compounds that significantly contributed to the discrimination of the different salinity classes for *M. aeruginosa*

PCC 7820 and PCC 7806 respectively. Among these potential biomarkers, 16 were common (i.e for variables having VIP scores > 1) to both strains while 19 were specific to *M. aeruginosa* PCC 7820 and 15 to *M. aeruginosa* PCC 7806.

Only some VIPs could be identified (Fig. 7). Among those showing a decreased relative expression with increasing salinity, we observed dmMC-LR for both strains (i.e. expression pattern in agreement with targeted analysis, Fig. 7A and B) and cyanopeptolin C but only in PCC 7806 (Fig. 7A). Concerning the biomarkers having an increased relative expression with increasing salinity, we notably confidently identified the second most important VIP in *M. aeruginosa* PCC 7820 as trehalose (Fig. 7B). However, the VIP corresponding to the same exact mass and retention time in *M. aeruginosa* PCC 7806 was sucrose. Trehalose and sucrose having the same exact mass were discriminated by their fragmentation patterns when compared to pure standards. Indeed, they yielded specific ion ratios: 365.1/203.05, 365.1/183.04 and 203.05/183.04 = 0.8, 2.3 and 2.7 for sucrose and 4.5, 102 and 23 for trehalose and spectra for PCC 7806 and 7820 matched accordingly (i.e. ratios 0.7, 1.9 and 2.7 vs. 3.9, 99 and 25, respectively). But trace presence of trehalose in PCC 7806 and sucrose in PCC 7820 cannot be totally excluded. In addition, several monogalactosyldiacylglycerol (MGDG) were putatively identified, namely MGDG (34:2) and (34:3) in PCC 7806 and MGDG (36:3) in both strains. MS/MS spectra were characteristic of galactolipids (e.g. galactose-derived neutral loss of 162 or 179, acylium ions and neutral losses corresponding to fatty acid moieties).

The relative cellular abundance of the VIPs was in general proportional to the salinities in both strains (Fig. 7).

Applied and Environmental Microbiology

Discussion

Salinity tolerance of *M. aeruginosa*

As *M. aeruginosa* has been reported to form blooms in brackish waters (11, 28), studying the response of acclimated strains of *M. aeruginosa* to higher salt concentration allowed to better assess the salinity tolerance of *M. aeruginosa*. After acclimation, the two strains presented distinct salinity tolerance up to 7.5 and 16.9 for *M. aeruginosa* PCC 7820 and PCC 7806 respectively, these salinities corresponding to freshwater environment up to mesohaline zones (5 < S < 18) (26). The strain PCC 7806 presented a wider range of tolerance in our culture conditions compared to the strain PCC 7820. This result could be explained by the origin of the strain (28, 38).

Our results are in agreement with field studies on the salinity tolerance of *Microcystis* (3, 20, 21, 30, 42). In our experiment, an increase in salinity led to a decrease of the growth rate for both strains, as well as a reduced cell size. Such a biovolume decrease has already been reported as a response to both gradually increasing salinity (29) and salt stress (31) for cyanobacteria. Tonk et al. (2007) considered this phenomenon as a consequence of the plasmolysis during their acclimation process. However, in our case, the biovolume decrease was observed even after acclimation. It was a long-term response compared to plasmolysis.

Impact of salinity on MC production

299 Factors influencing MC production as well as the inherent role of MCs are still under
300 debate (43). With the exception of one study (44), reports on the impact of salinity
301 variation concluded to a decrease of MC cellular quotas under higher salinity
302 conditions (23, 24, 29, 30). A decrease in MC cellular quota is frequently associated
303 with an increase in dissolved MC because of cell lysis (19, 23, 29). Our study also
304 showed that the MC cellular quota was decreased with increasing salinity for both
305 strains. In addition, a linear correlation was found between growth rate and net
306 production rate of MCs. This relation shows that MC cellular quotas in both strains
307 are strongly coupled to cell division, as already evidenced by Orr et al. (45).
308 Furthermore, as explained by Orr et al. (46), this correlation illustrates that salinity
309 only indirectly influences the production of MCs through its effect on growth. Also, as
310 a comparison, Amé and Wunderlin (2005) and Van de Waal et al. (2009), showed
311 that temperature and nutrients changed the MC congener ratios by up to a 82-fold
312 change. Our results suggested that salinity did not seem to alter the MC ratios in *M.*
313 *aeruginosa* in the same order of range. The extracellular MC fractions decreased
314 with time, indicating no significant cell lysis phenomenon. At high salinities, the higher
315 proportion of extracellular MCs resulted from the larger volume of inoculum. These
316 results suggest that no active excretion of MCs occurred in response to higher
317 salinities. Thus, the growth conditions were convenient for cell membrane integrity,
318 as well as showed by the stability of the maximum photochemical efficiency of
319 photosystem II over time. As a comparison, an active release of saxitoxin and
320 gonyautoxins 2 and 3 can be induced by sodium and potassium increase in
321 *Raphidiopsis* another toxic bloom forming cyanobacteria (49). Based on previous
322 studies (29, 50) and our results, the MCs did not appear to be accumulated in *M.*
323 *aeruginosa* cells in response to higher salinity. Overall, the growth of the two *M.*

aeruginosa strains was not restricted to freshwater conditions after acclimation. Therefore, our result confirm that this genus could be considered as a salt-tolerant cyanobacteria (6). Based on laboratory experiments, our results also support the recommendation that the intensification of *M. aeruginosa* blooms in brackish waters should be considered by the cyanobacteria harmful algal bloom monitoring programs worldwide (6, 28).

Targeted and non-targeted analyses of metabolites at different salinities

Using a metabolomic approach, this study describes the potential metabolites involved to sustain *M. aeruginosa* growth at high salinities. *M. aeruginosa* is considered as an organism using the “salt-out” strategy in response to an osmolarity of the external medium (51, 52). The “salt-out” strategy requires energy and organic matter for the accumulation of compatible solutes, which are used instead of inorganic ions to balance the osmotic potential and to maintain turgor (52). Compatible solutes can be accumulated in high molar amounts in the cells without negative impacts on the metabolism (53) and have a protective action on macromolecules (52). Herein, the metabolomic approach was applied to follow the evolution of the metabolome and identify biomarkers of salt acclimation. Firstly, both targeted and untargeted approaches showed that *M. aeruginosa* PCC 7820 and PCC 7806 possessed distinct metabolic profiles. Despite a non-negligible strain-specificity, it was possible to point out an evolution of metabolite profiles in response to the acclimation to distinct salinities. The consequences of the “salt-out” strategy as a costing energy strategy were illustrated in this study by a slower growth rate and a distinct metabolic profile at higher salinity compared to the control.

Among the diversity of metabolites detected in our experiment, the relative cellular quota of some compounds were over-expressed at higher salinity, suggesting that these compounds could be assimilated to compatible solutes. Two compounds identified in the literature as cyanobacterial osmolytes were detected: sucrose (mainly produced in PCC 7806) and trehalose (mainly produced in PCC 7820) (31). Kolman et al. (2012) found sucrose and the respective genes involved in its biosynthesis in *M. aeruginosa* PCC 7806. A sucrose accumulation in the cells was noticed after a hypoxic or a salt stress in PCC 7806 (37). After a recent work with new isolates of *M. aeruginosa* strains from brackish water, Tanabe et al. (2018) confirmed the importance of sucrose synthesis in the brackish strains, compared with the lack of sucrose genes and synthesis in the freshwater isolates. We identified sucrose as a VIP in *M. aeruginosa* PCC 7806, but we cannot exclude the presence of trehalose based on our LC-HRMS method (i.e same retention time and mass). Indeed, only one study did report the accumulation of trehalose in this strain in response to light intensity stress (54). On the other hand, trehalose but not sucrose (or only trace) was identified as a VIP in the less salt tolerant strain *M. aeruginosa* PCC 7820. Occurrence of trehalose is poorly documented in *M. aeruginosa*. Here, we pointed out a distinct response of these *M. aeruginosa* strains in response to salt acclimation. As reviewed by Hagemann (2011) for several other genera, the discrepancies in salt tolerance of *M. aeruginosa* strains could be partly explained by the accumulation of trehalose or sucrose.

As far as we know, a restricted number of studies reported the analyses of other identified compatible solutes using targeted analyses in *Microcystis* (36). DMSP is described as a constitutive compatible solute in some microalgae (32) and was found in low amounts in a few number of cyanobacteria genera (33). Based on our

373 analyses, DMSP was not detected in *M. aeruginosa*, corroborating the absence of
374 potentially released by-product DMS observed by Steinke et al. (2018). Targeted
375 analyses of GB and proline led us to quantify these compounds in *M. aeruginosa*
376 PCC 7820 and PCC 7806. GB and proline have been described as compatible
377 solutes in other genera of cyanobacteria (31). Salt stress-induced proline is
378 described for *E. coli*, diatoms and plants (55) while GB accumulation has long been
379 described in response to salt increase in heterotrophic bacteria, cyanobacteria and
380 plants (55). Our results confirmed that GB acts as a compatible solute for *M.*
381 *aeruginosa*. Both strains exhibited a decline of GB after 10 days, but this may be
382 compensated by other compatible solutes as GB in *Microcystis* belongs to a larger
383 pool of compatible solutes. Nevertheless, accumulation of GB appeared to be
384 specific to more halotolerant species than *M. aeruginosa*, e.g. species living in
385 hypersaline environment (56).
386 Metabolomic analyses led us to putatively identify cyanopeptolin C as a VIP of low
387 salinity in PCC 7806 while no trace of this compound was found in PCC 7820.
388 Cyanopeptolin C is a secondary metabolite already reported to be produced by PCC
389 7806 (57, 58). Besides evidence of inhibition activity on diverse human enzymes and
390 toxicity for grazers (59), limited data are available about the physiological role of
391 cyanopeptolin C in *Microcystis* cells. Abiotic factors such as temperature, light
392 intensity and phosphorus limitation influenced the amount of cyanopeptolin C per cell
393 in *M. aeruginosa* (60) but our experiment suggested that salinity could also be an
394 influencing factor. Using untargeted analyses led us to putatively identify
395 polyunsaturated glycolipids as VIP in both strains. MGDG (36:3) in PCC 7820 and
396 MGDG (34:2) and (34:3) in PCC 7806 were relatively overexpressed with increasing
397 salinity compared to the control conditions. MGDGs are prevalent lipids in

cyanobacterial cell and thylakoid membranes (61). As one of the major glycerolipids found in cyanobacteria (61) MGDG play an important role in structural stabilization and function of membranes. Membrane fluidity is strongly dependent of the lipid unsaturation degree and composition and its evolution is recognized as one of the mechanism involved in response to environmental fluctuation (62). Allakhverdiev et al. (1999) studied the salt tolerance of *Synechocystis* PCC 6803 by comparing wild and mutant strains, the latter did not contain polyunsaturated lipids. They concluded that the degree of unsaturation of fatty acids is involved in the tolerance of the photosynthetic machinery to salt stress. Moreover, this study pointed out that the activity and synthesis of the Na^+/H^+ antiporter system might be suppressed under salt stress condition. This effect appeared to be counteracted by the accumulation of unsaturated lipids (63). Up to now, the presence of genes coding for Na^+/H^+ antiporter in *M. aeruginosa* genomes appeared to be strain-dependent and correlated to salt tolerance (38) but no data are available about the lipid composition of *M. aeruginosa* in response to salt stress. Identification of MGDGs as VIP in *M. aeruginosa* in salt-acclimated strains suggested that these glycerolipids could be considered as salt acclimated biomarkers and involved in the tolerance of *M. aeruginosa* to elevated salinity. Besides the different VIP identified in this experiment, several others presented an expression pattern close to the definition of compatible solutes. However, exhaustive identification of the detected compounds in the metabolomic analyses remains challenging. Hence, this study pointed out a potential diversity of compatible solutes in the genus *Microcystis* which could explained the discrepancies observed in salt tolerance among the two strains.

Herein, we showed that salinity only affected MC production indirectly through a decrease in growth rate of both strains. Intraspecific variability in salinity tolerances

Applied and Environmental Microbiology

423 are reflected in metabolite profiles changes between the two strains. It was possible
424 to identify different metabolites overexpressed in response to an increase in salinity.
425 These two strains did not rely on the same mechanisms in response to elevated
426 salinity which illustrate the plasticity of *Microcystis aeruginosa* in long term adaptation
427 to brackish conditions. Our data provide new insights about the metabolites involved
428 in *Microcystis* acclimation to higher salinity. Also, short term experiments at higher
429 salinity would precise whether similar mechanisms are involved in *M. aeruginosa.*
430 Further experiments based on genetic approach and specific quantification of
431 supplementary osmolytes in several strains of *Microcystis* are needed to better
432 understand the diversity of osmolytes in this genus. At last, further investigations are
433 required to confirm another hypothesis made by Orr et al. (2004) suggesting that
434 toxic phenotypes could survive longer at higher salinities compared to the non-toxic
435 ones.
436

437 **Materials and methods**

438 **Organisms and culture conditions**

439 Two axenic and toxic *M. aeruginosa* strains, available from the Pasteur Culture
440 collection of Cyanobacteria (PCC; https://webext.pasteur.fr/cyanobacteria/) were
441 studied, the PCC 7820 and PCC 7806 strains. Both strains were isolated from
442 contrasting environment, the freshwater lake Balgaries (Scotland) and the brackish
443 water of Braakman reservoir (Netherlands), respectively for PCC 7820 and PCC
444 7806. Cells were routinely grown in $BG11_0^*$ which is a $BG11_0$ medium (64)
445 supplemented with $NaNO_3$ (2 mM) and $NaHCO_3$ (10 mM), at constant temperature
446 of 22 ± 0.6°C under a 12:12 h light:dark cycle using cool-white fluorescent tubes
447 (Philips) with 35 µmol photons m^{-2} s^{-1} illumination. Artificial seawater was made

448 with the addition of NaCl (450 mM), KCl (10 mM), $CaCl_2$ (9 mM), $MgCl_2$ ($6H_2O$)
449 (30mM) and $MgSO_4$ ($7H_2O$) (16mM) before nutrient enrichment to achieve the
450 $BG11_{0\ +\ salts}^{*}$ preparation (65). Hence, the different salinities used in this study were
451 obtained by mixing both media $BG11_0^{*}$ and salt enriched $BG11_{0\ +\ salts}^{*}$. Salinity was
452 checked using a conductivity meter Cond 3110 Set 1 (WTW).

453

454

455 **Acclimation**

456 Before starting the experiment, strains were progressively acclimated to different
457 salinities by transferring the culture after 20 days of growth (i.e. during the
458 exponential growth phase) into fresh media of higher salinity. After each new
459 transfer, salinity was increased by 2 units. This process was repeated until
460 reaching the likely maximal salinity tolerance of the two strains. At the end of the
461 acclimation process, cultures were maintained between 25 and 50 generations at
462 each salinity. At least three constant growth rates confirmed the acclimation of the
463 strains in agreement with MacIntyre and Cullen (2005). Hence, *M. aeruginosa* PCC
464 7820 and PCC 7806 were acclimated respectively to 3 salinities (3.7, 6.4 and 7.5)
465 and 7 salinities (3.6, 6.0, 8.4, 10.7, 12.2, 14.8 and 16.9), in addition to the control
466 culture condition in $BG11_0^{*}$ (S = 0.6).

467

468 **Experiment**

469 Once acclimated to each salinity, both strains were maintained in batch culture and
470 transferred to new fresh medium during exponential growth phase. Therefore,
471 triplicate batch cultures in 300 mL flask were inoculated at 1 x 10^6 cells mL^{-1} with

exponential growing cells and maintained under temperature and light conditions described above during 30 days.

Sampling and analyses

Growth rate

Cell concentration was monitored every two days. Samples (2 mL) were fixed with glutaraldehyde (0.1%) (Sigma-Aldrich) and stored at -80°C until analyses on an Accuri C6 flow cytometer (Becton Dickinson) (67). Growth rate (μ) was calculated during exponential growth using least-squares regression method (68). Furthermore, the forward scatter fluorescence (FSC) was used to compare the mean relative cell size between salinities on sampling day 14 only (i.e. during mid-exponential growth phase).

Maximum photochemical efficiency of photosystem II

Maximum quantum efficiency of the photosystem II (F_v/F_m) was measured after 4, 10, 14 and 24 days using an Aquapen-C 100 fluorimeter (Photon Systems Instruments). Before fluorescence analyses, samples (3 mL) were incubated in the dark for 15 min (69).

Microcystin analyses

To determine the intra- and extracellular toxin contents after 4, 10, 14 and 24 days, samples (15 mL) were harvested and centrifuged at 4248 g for 15 min at 4°C. The

supernatant was directly stored at -80°C and the remaining cell pellet was quenched in liquid nitrogen and stored at -80°C until extraction. For the extraction of intracellular toxins, 250 mg of glass beads (0.15 - 0.25 mm, VWR) and 1 mL of methanol (Honeywell) were added to the pellet before mechanical grinding using a mixer mill (MM400, Retsch) during 30 min at 30 Hz. Tubes were centrifuged at 13000 g and supernatants were filtered through 0.2 µm filter (Nanosep MF, Pall). Extracellular MCs were extracted by solid phase extraction (200 mg Bond Elut C18 cartridges, Agilent) to remove salts and concentrate the MCs. After conditioning with 3 mL of MeOH and 3 mL of Milli-Q water, 15 mL of cell-free medium were loaded, rinsed with 2.4 mL of MeOH/Milli-Q water (5:95, v/v) and eluted with 4 mL of MeOH. Subsequently, intracellular and extracellular MC analyses were performed by ultra-fast liquid chromatography (Nexera, Shimadzu), coupled to a triple quadrupole mass spectrometer (5500 QTrap, ABSciex) equipped with a TurboV® electrospray ionization source (LC-MS/MS). The analytical chomatographic column was a Kinetex XB C18 (100x2.1 mm, 2.6 µm, Phenomenex) equipped with a suited guard column. The column and sample temperatures were 25°C and 4°C. The flow rate was 0.3 mL min^{-1} and the volume of injection 5 µL. The binary gradient consisted of water (A) and acetonitrile (B), both containing 0.1% formic acid (v/v). The elution gradient was: 30-80% B (0-5 min), 80% B (5-6 min), 30% B (6.5-10.5 min). MS/MS detection was performed in positive ionization mode using multiple reaction monitoring (MRM) with two transitions per toxin (Table S1). Nine certified MC standards (Novakits) were used to quantify MC content in both intracellular and extracellular fractions, using an external 6-points calibration curve. Acquisition and data processing were performed using Analyst 1.6.3 (ABSciex) software. Total recoveries (i.e. combining

Applied and Environmental Microbiology

extraction recovery and remaining matrix effect when spiking before extraction) were evaluated for intracellular and extracellular MC quantifications (Tables S3 and S4). Intracellular MC recoveries were higher than 93% and extracellular MC recoveries were similar between a medium with and without salt for (with differences of 3-9%) (Tables S3 and S4). Therefore no corrective factor was applied. The net production rate of each MC variant was calculated according to the method described by Orr et al. (45) by application of first order rate kinetics.

DMSP, GB and proline analyses

DMSP, GB and proline quantifications were measured by LC-MS/MS on intracellular cell extracts prepared for toxin analysis on a LC System (model UFLC XR, Shimadzu) coupled to a triple quadrupole mass spectrometer (4000 QTrap, ABSciex). Chromatography was performed with a Hypersil GOLD HILIC column (150 × 3.0 mm, 3 µm, ThermoScientific) with a suited guard column, based on Curson et al. (2018). The binary gradient consisted of water/ACN (90:10; V/V) containing 4.5 mM ammonium formate (A) and water (5:95; V/V) containing 5 mM ammonium formate (B). The flow rate was 0.4 mL min^{-1} and injection volume was 5 µL. The column and sample temperatures were 30°C and 4°C, respectively. The elution gradient was 90% B (0-1 min), 90-45% B (1-8 min), 45% B (8-12 min), 90% B (12-15 min). The LC-MS/MS system was used in positive ionization mode and MRM, with the two transitions per compounds (Table S2). Compounds were quantified using an external 5-point calibration curves of standards (Sigma Aldrich) solubilized in methanol, with concentrations from 50 nM to 5000 nM. Acquisition and data processing were performed using Analyst 1.6.3 (ABSciex) software. Total

545 extraction recoveries were evaluated between strains and salt conditions (Table S5).
546 As total recoveries did not vary more than 20% between control condition (S = 0.6)
547 and maximum conditions for both strains (S = 7.5 and 16.9), the quantification results
548 were not corrected (Table S5).
549
550
551
552
553
554 **Metabolomic analysis**
555
556 **Data acquisition**
557 Metabolomic analysis was only conducted on intracellular extracts prepared for toxin
558 analysis at day 14 (i.e. during mid-exponential growth phase). Metabolomic profiles
559 were acquired by Ultra-performance Liquid Chromatography – High Resolution Mass
560 Spectrometry (UPLC-HRMS). The instrumentation consisted of a UHPLC system
561 (1290 Infinity II, Agilent) coupled to a quadrupole-time of flight mass spectrometer
562 (QTOF 6550, Agilent) equipped with a Dual Jet Stream electrospray ionization (ESI)
563 interface. Analyses were carried out using an analytical core-shell Phenyl-hexyl
564 column (150 x 2.1 mm, 1.7 µm, Phenomenex) with a suited guard column. The
565 column and sample temperatures were 40°C and 4°C, respectively. The flow rate
566 was 0.5 mL min^{-1} and the injection volume was 5 µL. Mobile phases consisted of
567 water (A) and acetonitrile (B), both containing 0.1 formic acid (v/v). The following
568 elution gradient was used: 5% B (0-2 min), 5-100% B (2-10 min), 100% B (10-14
569 min), 5% B (14-18 min). Mass spectra were recorded in full-scan mode from *m/z* 100

570 to 1700 (500 ms scan time) at a mass resolving power of 25000 full width at half-
571 maximum (fwhm, *m/z* = 922.0099) and an acquisition rate of 2 spectra s^{-1}. A
572 calibration-check was performed continuously over the entire run time using
573 reference masses *m/z* 121.0509 (purine) and *m/z* 922.0099 (hexakis phosphazine).
574 Samples were randomly injected. Pool samples (QC) were prepared and injected ten
575 times at the beginning of the batch sequence and then every four samples (including
576 blank). Blanks were prepared as cell pellets (i.e. MeOH and glass beads in a
577 polypropylene tube). Data were deposited on DATAREF
578 (https://doi.org/10.12770/414f1f4c-5f1c-4e98-a187-c66216393d6e). To identify
579 specific compounds of interest, tandem mass spectrometry analyses were carried out
580 at an acquisition rate of 5 spectra s^{-1} for MS (*m/z* 100 – 1700, 200 ms scan time) and
581 15 spectra s^{-1} for MS/MS (*m/z* 50 – 1700, 66.7 ms scan time). Collision-induced
582 dissociation was performed on the 3 most intense ions above an absolute threshold
583 of 2000 counts. A collision energy value proportional to the *m/z* of the selected
584 precursor ion, an isolation window of 1.3 amu and a dynamic exclusion time of 30 s
585 were used. Annotation was conducted firstly with exact masses and freely available
586 databases (e.g. HMDB, LipidMaps, Metlin, KEGG, http://ceumass.eps.uspceu.es/),
587 Gil-de-la-Fuente et al. 2019)) then with fragmentation patterns and using a molecular
588 networking approach (https://gnps.ucsd.edu/, (72)). Acquisition and data processing
589 were performed using Mass Hunter Workstation softwares (version B.06.01 and
590 B.07, Agilent).
591
592 **Data pre-processing and filtering**
593 LC-MS raw data (.d) were converted to .mzXML format using MS-Convert
594 (Proteowizard 3.0, (73)) and processed with the XCMS package (74) under R 3.2.3

environment. Peak picking was performed with the “centWave” algorithm, retention time correction with the “obiwarp” algorithm, peak grouping with “bw” = 5 and “mzwid” = 0.015 and peak filling with the default parameters.

Three successive filtering steps using in-house scripts on R were applied to remove (i) variables with low intensities (exclusion of variables with S/N <10 compared to a blank), (ii) signals showing high variability (exclusion of variables with a coefficient of variation >20% in QC samples) and (iii) to suppress redundancy (exclusion of all variables but the most intense one when the coefficient of autocorrelation >80% at the same retention time). Pre-processing led to 298 variables and 83 variables remained after the filtrations on which statistical analyses were performed.

Statistical analyses

Statistical analyses of the data were performed using R software (R core team). Data are presented as mean and standard deviation (SD). After checking the homoscedasticity and normal distribution of residuals using Bartlett and Shapiro-Wilk tests, the effect of salinity on growth was tested using one-way analysis of variance (ANOVA) and the post-hoc Dunnett’s test was applied to check a difference between growth rates (in comparison to the control). Otherwise, if the hypothesis of normal distribution and homoscedasticity of residuals were not verified a non-parametric Kruskal-Wallis test was performed. The impact of salinity and time on the individual MC congener quotas were checked by performing two-way ANOVAs. Two-way ANOVA on repeated measures with time as the within subjects factor and the salinity as the between subjects factor were conducted.The Pearson’s correlation coefficient was calculated between growth rates and net production rates of MCs. For metabolomics, multivariate statistical analyses were performed using MetaboAnalyst 4.0. (75). First, as different amount of cells were extracted depending on salinity

conditions, the data were normalized to cell concentration as a sample-specific normalization. Then, data were log transformed and Pareto scaled based on the recommendation of Van den Berg et al. (2006). Principal component analysis (PCA) and partial least-square discriminant analysis (PLS-DA) were used. The PLS-DA models were validated using a permutation test (Separation distance: B/W, 1000 permutations, p-values < 0.007) and allowed us to highlight discriminant metabolites using the variable importance in projection (VIP) score commonly used for biomarker selection, assuming that a VIP score >1 corresponded to a 'biomarker'.

Acknowledgments

The authors acknowledge Ifremer and the Regional Council of the *Région des Pays de la Loire* for the PhD funding of Maxime Georges des Aulnois.

645
646
647
648
649
650
651
652
653
654

655 **References**

656 1. O'Neil JM, Davis TW, Burford MA, Gobler CJ. 2012. The rise of harmful
657 cyanobacteria blooms: The potential roles of eutrophication and climate
658 change. Harmful Algae 14:313–334.
659 2. Nielsen DL, Brock MA, Rees GN, Baldwin DS. 2003. Effects of increasing
660 salinity on freshwater ecosystems in Australia. Aust J Bot 51:655.
661 3. Verspagen JMH, Passarge J, Jöhnk KD, Visser PM, Peperzak L, Boers P,
662 Laanbroek HJ, Huisman J. 2006. Water management strategies against toxic
663 Microcystis blooms in the Dutch delta. Ecol Appl 16:313–27.
664 4. White E, Kaplan D. 2017. Restore or retreat? saltwater intrusion and water
665 management in coastal wetlands. Ecosyst Heal Sustain 3:e01258.
666 5. Huisman J, Codd GA, Paerl HW, Ibelings BW, Verspagen JMH, Visser PM.
667 2018. Cyanobacterial blooms. Nat Rev Microbiol 16:471–483.
668 6. Paerl HW, Huisman J. 2009. Climate change: a catalyst for global expansion of
669 harmful cyanobacterial blooms. Environ Microbiol Rep 1:27–37.

7. Paerl H. 2014. Mitigating Harmful Cyanobacterial Blooms in a Human- and Climatically-Impacted World. Life 4:988–1012.

8. Funari E, Manganelli M, Buratti FM, Testai E. 2017. Cyanobacteria blooms in water: Italian guidelines to assess and manage the risk associated to bathing and recreational activities. Sci Total Environ 598:867–880.

9. Harke MJ, Steffen MM, Gobler CJ, Otten TG, Wilhelm SW, Wood SA, Paerl HW. 2016. A review of the global ecology, genomics, and biogeography of the toxic cyanobacterium, Microcystis spp. Harmful Algae 54:4–20.

10. Humbert J-F, Barbe V, Latifi A, Gugger M, Calteau A, Coursin T, Lajus A, Castelli V, Oztas S, Samson G, Longin C, Medigue C, de Marsac NT. 2013. A Tribute to Disorder in the Genome of the Bloom-Forming Freshwater Cyanobacterium Microcystis aeruginosa. PLoS One 8:e70747.

11. Preece EP, Hardy FJ, Moore BC, Bryan M. 2017. A review of microcystin detections in Estuarine and Marine waters: Environmental implications and human health risk. Harmful Algae 61:31–45.

12. Robson BJ, Hamilton DP. 2003. Summer flow event induces a cyanobacterial bloom in a seasonal Western Australian estuary. Mar Freshw Res 54:139.

13. Takahashi T, Umehara A, Tsutsumi H. 2014. Diffusion of microcystins (cyanobacteria hepatotoxins) from the reservoir of Isahaya Bay, Japan, into the marine and surrounding ecosystems as a result of large-scale drainage. Mar Pollut Bull 89:250–258.

14. Preece EP, Moore BC, Hardy FJ. 2015. Transfer of microcystin from freshwater lakes to Puget Sound, WA and toxin accumulation in marine mussels (Mytilus trossulus). Ecotoxicol Environ Saf 122:98–105.

15. Martínez de la Escalera G, Kruk C, Segura AM, Nogueira L, Alcántara I, Piccini

C. 2017. Dynamics of toxic genotypes of Microcystis aeruginosa complex (MAC) through a wide freshwater to marine environmental gradient. Harmful Algae 62:73–83.

16. Lehman PW, Kurobe T, Lesmeister S, Baxa D, Tung A, Teh SJ. 2017. Impacts of the 2014 severe drought on the Microcystis bloom in San Francisco Estuary. Harmful Algae 63:94–108.

17. Bormans M, Amzil Z, Mineaud E, Brient L, Savar V, Robert E, Lance E. 2019. Demonstrated transfer of cyanobacteria and cyanotoxins along a freshwater-marine continuum in France. Harmful Algae 87:101639.

18. Paerl HW, Otten TG, Kudela R. 2018. Mitigating the Expansion of Harmful Algal Blooms Across the Freshwater-to-Marine Continuum. Environ Sci Technol 52:5519–5529.

19. Ross C, Warhurst BC, Brown A, Huff C, Ochrietor JD. 2019. Mesohaline conditions represent the threshold for oxidative stress, cell death and toxin release in the cyanobacterium Microcystis aeruginosa. Aquat Toxicol 206:203–211.

20. Otsuka S, Suda S, Li R, Watanabe M, Oyaizu H, Matsumoto S, Watanabe and MM. 1999. Characterization of morphospecies and strains of the genus Microcystis (Cyanobacteria) for a reconsideration of species classification. Phycol Res 47:189–197.

21. Orr PT, Jones GJ, Douglas GB. 2004. Response of cultured Microcystis aeruginosa from the Swan River, Australia, to elevated salt concentration and consequences for bloom and toxin management in estuaries. Mar Freshw Res 55:277.

22. Bartolomé MC, D'ors A, Sánchez-Fortún S. 2009. Toxic effects induced by salt

stress on selected freshwater prokaryotic and eukaryotic microalgal species. Ecotoxicology 18:174–179.

23. Black K, Yilmaz M, Phlips EJ. 2011. Growth and Toxin Production by Microcystis Aeruginosa PCC 7806 (Kutzing) Lemmerman at Elevated Salt Concentrations. J Environ Prot (Irvine, Calif) 02:669–674.

24. Martín-Luna B, Sevilla E, Bes MT, Fillat MF, Peleato ML. 2015. Variation in the synthesis of microcystin in response to saline and osmotic stress in Microcystis ruginosa PCC7806. Limnetica 34:205–214.

25. Reed RH, Walsby AE. 1985. Changes in turgor pressure in response to increases in external NaCl concentration in the gas-vacuolate cyanobacterium Microcystis sp. Arch Microbiol 143:290–296.

26. Mitsch WJ, Gosselink JG. 2000. Wetlands john wiley & sons. Inc, New York, New York.

27. Zhang Y, Xu Q, Xi B. 2013. Effect of NaCl salinity on the growth, metabolites, and antioxidant system of Microcystis aeruginosa. J Freshw Ecol 28:477–487.

28. Tanabe Y, Hodoki Y, Sano T, Tada K, Watanabe MM. 2018. Adaptation of the Freshwater Bloom-Forming Cyanobacterium Microcystis aeruginosa to Brackish Water Is Driven by Recent Horizontal Transfer of Sucrose Genes. Front Microbiol 9:1–11.

29. Tonk L, Bosch K, Visser P, Huisman J. 2007. Salt tolerance of the harmful cyanobacterium Microcystis aeruginosa. Aquat Microb Ecol 46:117–123.

30. Mazur-Marzec H, Forycka K, Kobos J, Pliński M, Browarczyk-Matusiak G. 2010. Morphological, genetic, chemical and ecophysiological characterisation of two Microcystis aeruginosa isolates from the Vistula Lagoon, southern Baltic. OCEANOLOGIA 52:127–146.

31. Hagemann M. 2011. Molecular biology of cyanobacterial salt acclimation. FEMS Microbiol Rev 35:87–123.

32. Stefels J. 2000. Physiological aspects of the production and conversion of DMSP in marine algae and higher plants. J Sea Res 43:183–197.

33. Oren A. 2007. Diversity of Organic Osmotic Compounds and Osmotic Adaptation in Cyanobacteria and Algae, p. 639–655. *In* Archaea.

34. Bucciarelli E, Ridame C, Sunda WG, Dimier-Hugueney C, Cheize M, Belviso S. 2013. Increased intracellular concentrations of DMSP and DMSO in iron-limited oceanic phytoplankton Thalassiosira oceanica and Trichodesmium erythraeum. Limnol Oceanogr 58:1667–1679.

35. Steinke M, Hodapp B, Subhan R, Bell TG, Martin-Creuzburg D. 2018. Flux of the biogenic volatiles isoprene and dimethyl sulfide from an oligotrophic lake. Sci Rep 8:630.

36. Hagemann M, Erdmann N, Wittenburg E. 1987. Synthesis of glucosylglycerol in salt-stressed cells of the cyanobacterium Microcystis firma. Arch Microbiol 148:275–279.

37. Kolman MA, Torres LL, Martin ML, Salerno GL. 2012. Sucrose synthase in unicellular cyanobacteria and its relationship with salt and hypoxic stress. Planta 235:955–964.

38. Sandrini G, Huisman J, Matthijs HCP. 2015. Potassium sensitivity differs among strains of the harmful cyanobacterium Microcystis and correlates with the presence of salt tolerance genes. FEMS Microbiol Lett 362:1–17.

39. Szymańska E, Saccenti E, Smilde AK, Westerhuis JA. 2012. Double-check: validation of diagnostic statistics for PLS-DA models in metabolomics studies. Metabolomics 8:3–16.

770 40. Favre L, Ortalo-Magné A, Pichereaux C, Gargaros A, Burlet-Schiltz O, Cotelle
771 V, Culioli G. 2018. Metabolome and proteome changes between biofilm and
772 planktonic phenotypes of the marine bacterium Pseudoalteromonas lipolytica
773 TC8. Biofouling 34:132–148.
774 41. Lê Cao K-A, Boitard S, Besse P. 2011. Sparse PLS discriminant analysis:
775 biologically relevant feature selection and graphical displays for multiclass
776 problems. BMC Bioinformatics 12:253.
777 42. Atkins R, Rose T, Brown RS, Robb M. 2001. The Microcystis cyanobacteria
778 bloom in the Swan River - February 2000. Water Sci Technol 43:107–114.
779 43. Omidi A, Esterhuizen-Londt M, Pflugmacher S. 2018. Still challenging: the
780 ecological function of the cyanobacterial toxin microcystin – What we know so
781 far. Toxin Rev 37:87–105.
782 44. Chen L, Mao F, Kirumba GC, Jiang C, Manefield M, He Y. 2015. Changes in
783 metabolites, antioxidant system, and gene expression in Microcystis
784 aeruginosa under sodium chloride stress. Ecotoxicol Environ Saf 122:126–135.
785 45. Orr PT, Willis A, Burford MA. 2018. Application of first order rate kinetics to
786 explain changes in bloom toxicity—the importance of understanding cell toxin
787 quotas. J Oceanol Limnol 36:1063–1074.
788 46. Orr PT, Jones GJ. 1998. Relationship between microcystin production and cell
789 division rates in nitrogen-limited Microcystis aeruginosa cultures. Limnol
790 Oceanogr 43:1604–1614.
791 47. Amé MV, Wunderlin DA. 2005. Effects of Iron, Ammonium and Temperature on
792 Microcystin Content by a Natural Concentrated Microcystis Aeruginosa
793 Population. Water Air Soil Pollut 168:235–248.
794 48. Van de Waal DB, Verspagen JMH, Lürling M, Van Donk E, Visser PM,

Huisman J. 2009. The ecological stoichiometry of toxins produced by harmful cyanobacteria: an experimental test of the carbon-nutrient balance hypothesis. Ecol Lett 12:1326–1335.

49. Soto-Liebe K, Méndez MA, Fuenzalida L, Krock B, Cembella A, Vásquez M. 2012. PSP toxin release from the cyanobacterium Raphidiopsis brookii D9 (Nostocales) can be induced by sodium and potassium ions. Toxicon 60:1324–1334.

50. Sevilla E, Martin-Luna B, Bes MT, Fillat MF, Peleato ML. 2012. An active photosynthetic electron transfer chain required for mcyD transcription and microcystin synthesis in Microcystis aeruginosa PCC7806. Ecotoxicology 21:811–819.

51. Galinski E A. 1995. Osmoadaptation in bacteriaAdvances in Microbial Physiology.

52. Hagemann M. 2013. Genomics of Salt Acclimation, p. 27–55. *In* BS:ABR. Elsevier.

53. Brown AD. 1976. Microbial water stress. Bacteriol Rev 40:803–46.

54. Meissner S, Steinhauser D, Dittmann E. 2015. Metabolomic analysis indicates a pivotal role of the hepatotoxin microcystin in high light adaptation of M icrocystis. Environ Microbiol 17:1497–1509.

55. Hagemann M. 2016. The Physiology of MicroalgaeThe Physiology of Microalgae. Springer International Publishing, Cham.

56. Klähn S, Hagemann M. 2011. Compatible solute biosynthesis in cyanobacteria. Environ Microbiol 13:551–562.

57. Martin C, Oberer L, Ino T, König WA, Busch M, Weckesser J. 1993. Cyanopeptolins, new depsipeptides from the cyanobacterium Microcystis sp.

pcc 7806. J Antibiot (Tokyo) 46:1550–1556.

58. Briand E, Bormans M, Gugger M, Dorrestein PC, Gerwick WH. 2016. Changes in secondary metabolic profiles of Microcystis aeruginosa strains in response to intraspecific interactions. Environ Microbiol 18:384–400.

59. Janssen EML. 2019. Cyanobacterial peptides beyond microcystins – A review on co-occurrence, toxicity, and challenges for risk assessment. Water Res 151:488–499.

60. Tonk L, Welker M, Huisman J, Visser PM. 2009. Production of cyanopeptolins, anabaenopeptins, and microcystins by the harmful cyanobacteria Anabaena 90 and Microcystis PCC 7806. Harmful Algae 8:219–224.

61. Wada H, Murata N. 1998. Membrane Lipids in Cyanobacteria BT - Lipids in Photosynthesis: Structure, Function and Genetics, p. 65–81. *In* Paul-André, S, Norio, M (eds.), . Springer Netherlands, Dordrecht.

62. Mikami K, Murata N. 2003. Membrane fluidity and the perception of environmental signals in cyanobacteria and plants. Prog Lipid Res 42:527–543.

63. Allakhverdiev SI, Nishiyama Y, Suzuki I, Tasaka Y, Murata N. 1999. Genetic engineering of the unsaturation of fatty acids in membrane lipids alters the tolerance of Synechocystis to salt stress. Proc Natl Acad Sci 96:5862–5867.

64. Rippka R, Deruelles J, Waterbury JB, Herdman M, Stanier RY. 1979. Generic assignments, strain histories and properties of pure cultures of cyanobacteria. Microbiology 111:1–61.

65. Bail A Le, Charrier B. 2013. Plant Organogenesis. Humana Press, Totowa, NJ.

66. MacIntyre HL, Cullen JJ. 2005. Using cultures to investigate the physiological ecology of microalgae. Algal Cult Tech 287–326.

67. Marie D, Simon N, Vaulot D. 2005. Phytoplankton cell counting by flow

845 cytometry. Algal Cult Tech 1:253–267.
846 68. Wood AM, Everroad RC, Wingard LM. 2005. Measuring growth rates in
847 microalgal cultures. Algal Cult Tech 18:269–288.
848 69. Kromkamp JC, Forster RM. 2003. The use of variable fluorescence
849 measurements in aquatic ecosystems: differences between multiple and single
850 turnover measuring protocols and suggested terminology. Eur J Phycol
851 38:103–112.
852 70. Curson ARJ, Williams BT, Pinchbeck BJ, Sims LP, Martínez AB, Rivera PPL,
853 Kumaresan D, Mercadé E, Spurgin LG, Carrión O. 2018. DSYB catalyses the
854 key step of dimethylsulfoniopropionate biosynthesis in many phytoplankton.
855 Nat Microbiol 3:430.
856 71. Gil-de-la-Fuente A, Godzien J, Saugar S, Garcia-Carmona R, Badran H,
857 Wishart DS, Barbas C, Otero A. 2019. CEU Mass Mediator 3.0: A Metabolite
858 Annotation Tool. J Proteome Res 18:797–802.
859 72. Wang M, Carver JJ, Phelan V V., Sanchez LM, Garg N, Peng Y, Nguyen DD,
860 Watrous J, Kapono CA, Luzzatto-Knaan T, Porto C, Bouslimani A, Melnik A V.,
861 Meehan MJ, Liu W-T, Crüsemann M, Boudreau PD, Esquenazi E, Sandoval-
862 Calderón M, Kersten RD, Pace LA, Quinn RA, Duncan KR, Hsu C-C, Floros
863 DJ, Gavilan RG, Kleigrewe K, Northen T, Dutton RJ, Parrot D, Carlson EE,
864 Aigle B, Michelsen CF, Jelsbak L, Sohlenkamp C, Pevzner P, Edlund A,
865 McLean J, Piel J, Murphy BT, Gerwick L, Liaw C-C, Yang Y-L, Humpf H-U,
866 Maansson M, Keyzers RA, Sims AC, Johnson AR, Sidebottom AM, Sedio BE,
867 Klitgaard A, Larson CB, Boya P CA, Torres-Mendoza D, Gonzalez DJ, Silva
868 DB, Marques LM, Demarque DP, Pociute E, O'Neill EC, Briand E, Helfrich
869 EJN, Granatosky EA, Glukhov E, Ryffel F, Houson H, Mohimani H, Kharbush

JJ, Zeng Y, Vorholt JA, Kurita KL, Charusanti P, McPhail KL, Nielsen KF, Vuong L, Elfeki M, Traxler MF, Engene N, Koyama N, Vining OB, Baric R, Silva RR, Mascuch SJ, Tomasi S, Jenkins S, Macherla V, Hoffman T, Agarwal V, Williams PG, Dai J, Neupane R, Gurr J, Rodríguez AMC, Lamsa A, Zhang C, Dorrestein K, Duggan BM, Almaliti J, Allard P-M, Phapale P, Nothias L-F, Alexandrov T, Litaudon M, Wolfender J-L, Kyle JE, Metz TO, Peryea T, Nguyen D-T, VanLeer D, Shinn P, Jadhav A, Müller R, Waters KM, Shi W, Liu X, Zhang L, Knight R, Jensen PR, Palsson BØ, Pogliano K, Linington RG, Gutiérrez M, Lopes NP, Gerwick WH, Moore BS, Dorrestein PC, Bandeira N. 2016. Sharing and community curation of mass spectrometry data with Global Natural Products Social Molecular Networking. Nat Biotechnol 34:828–837.

73. Chambers MC, Maclean B, Burke R, Amodei D, Ruderman DL, Neumann S, Gatto L, Fischer B, Pratt B, Egertson J, Hoff K, Kessner D, Tasman N, Shulman N, Frewen B, Baker TA, Brusniak M-Y, Paulse C, Creasy D, Flashner L, Kani K, Moulding C, Seymour SL, Nuwaysir LM, Lefebvre B, Kuhlmann F, Roark J, Rainer P, Detlev S, Hemenway T, Huhmer A, Langridge J, Connolly B, Chadick T, Holly K, Eckels J, Deutsch EW, Moritz RL, Katz JE, Agus DB, MacCoss M, Tabb DL, Mallick P. 2012. A cross-platform toolkit for mass spectrometry and proteomics. Nat Biotechnol 30:918–920.

74. Smith CA, Want EJ, O'Maille G, Abagyan R, Siuzdak G. 2006. XCMS: processing mass spectrometry data for metabolite profiling using nonlinear peak alignment, matching, and identification. Anal Chem 78:779–787.

75. Chong J, Soufan O, Li C, Caraus I, Li S, Bourque G, Wishart DS, Xia J. 2018. MetaboAnalyst 4.0: towards more transparent and integrative metabolomics analysis. Nucleic Acids Res 46:W486–W494.

76. van den Berg RA, Hoefsloot HCJ, Westerhuis JA, Smilde AK, van der Werf MJ. 2006. Centering, scaling, and transformations: Improving the biological information content of metabolomics data. BMC Genomics 7:1–15.

77. Sumner LW, Amberg A, Barrett D, Beale MH, Beger R, Daykin CA, Fan TW-M, Fiehn O, Goodacre R, Griffin JL, Hankemeier T, Hardy N, Harnly J, Higashi R, Kopka J, Lane AN, Lindon JC, Marriott P, Nicholls AW, Reily MD, Thaden JJ, Viant MR. 2007. Proposed minimum reporting standards for chemical analysis Chemical Analysis Working Group (CAWG) Metabolomics Standards Initiative (MSI). Metabolomics 3:211–221.

Figure legends

FIG 1: Cell concentrations over time for both strains at each salinity condition. (A: *Microcystis aeruginosa* PCC 7820, B: *Microcystis aeruginosa* PCC 7806). Circles represent means and error bars represent the standard deviations from triplicate cultures.

FIG 2: Mean growth rate obtained during the exponential growth phase, calculated for each salinity and on each triplicate of culture (A: *Microcystis aeruginosa* PCC 7820, B: *Microcystis aeruginosa* PCC 7806). * Significantly different to the control condition (salinity 0.6), $p < 0.05$ (Dunnett test). Black circles represent means and error bars represent the standard deviations.

FIG 3 A: Microcystin cellular quotas (including MC-LR, MC-LW, MC-LF, MC-LY, dmMC-LR) over time and salinities for *M. aeruginosa* PCC 7820 and B: for *M. aeruginosa* PCC 7806 (MC-LR and dmMC-LR). Error bars represent the standard deviations (n = 3).

FIG 4 A: Proportions of intracellular and extracellular MCs over time and salinities for *M. aeruginosa* PCC 7820 and B for *M. aeruginosa* PCC 7806.

FIG 5 A: GB and proline cellular quotas over time and salinities for *M. aeruginosa* PCC 7820 and B: for PCC 7806. Error bars represent the standard deviations (n = 3). A lack of histogram bar means that the amount of compounds was below the detection limit.

FIG 6 PCA score plot obtained from UPLC-HRMS profiles for both strains and all tested salinities.

FIG 7 Details about the VIPs detected for PCC 7820 (A) and PCC 7806 (B). For each VIP, the VIP score, the ratio *m/z*, the retention time on the HPLC column, the putative identification (ID) and the relative cellular quota as a heatmap representation are presented. NA: Compound not identified. A green color expressed a relative lower cellular quota of a compound a sample compare to the others. Levels 1 and 2 refer to Sumner et al. (2007) and provide a confidence level for the ID of the VIP.

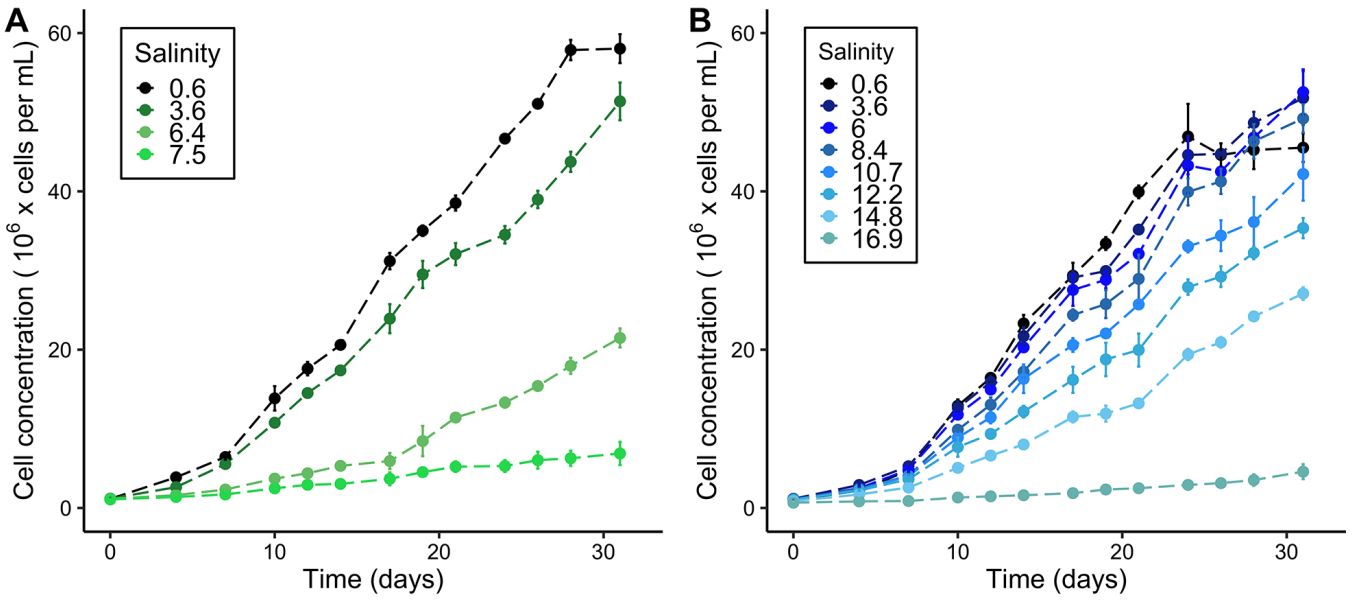

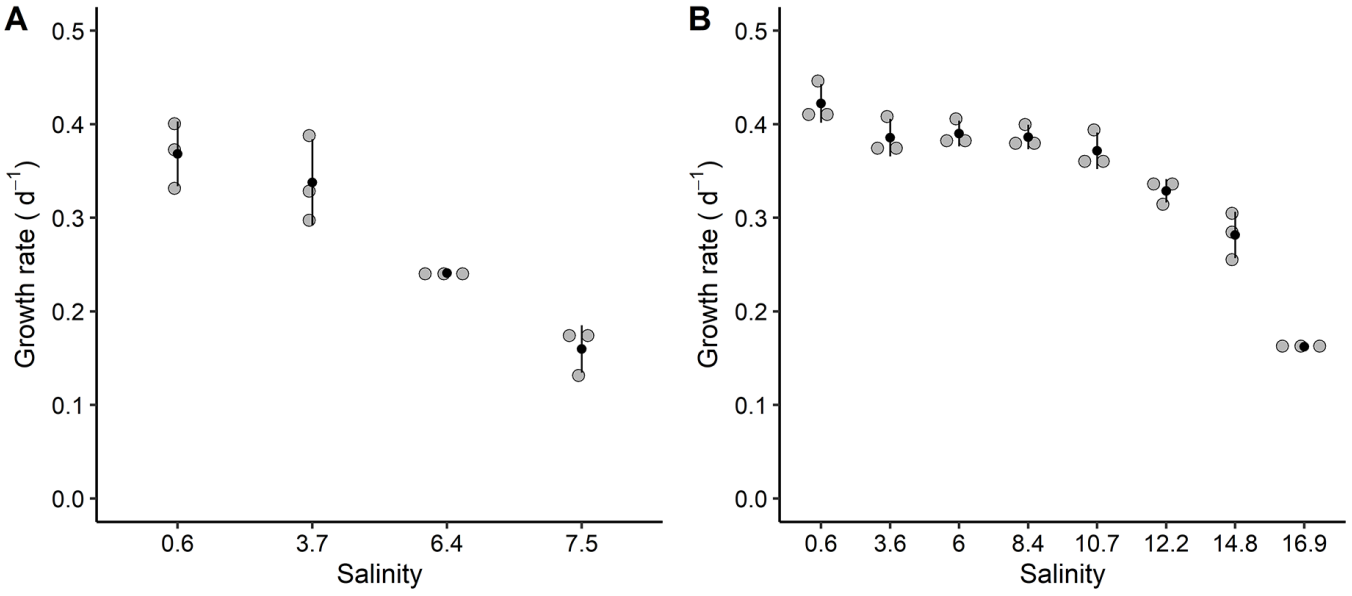

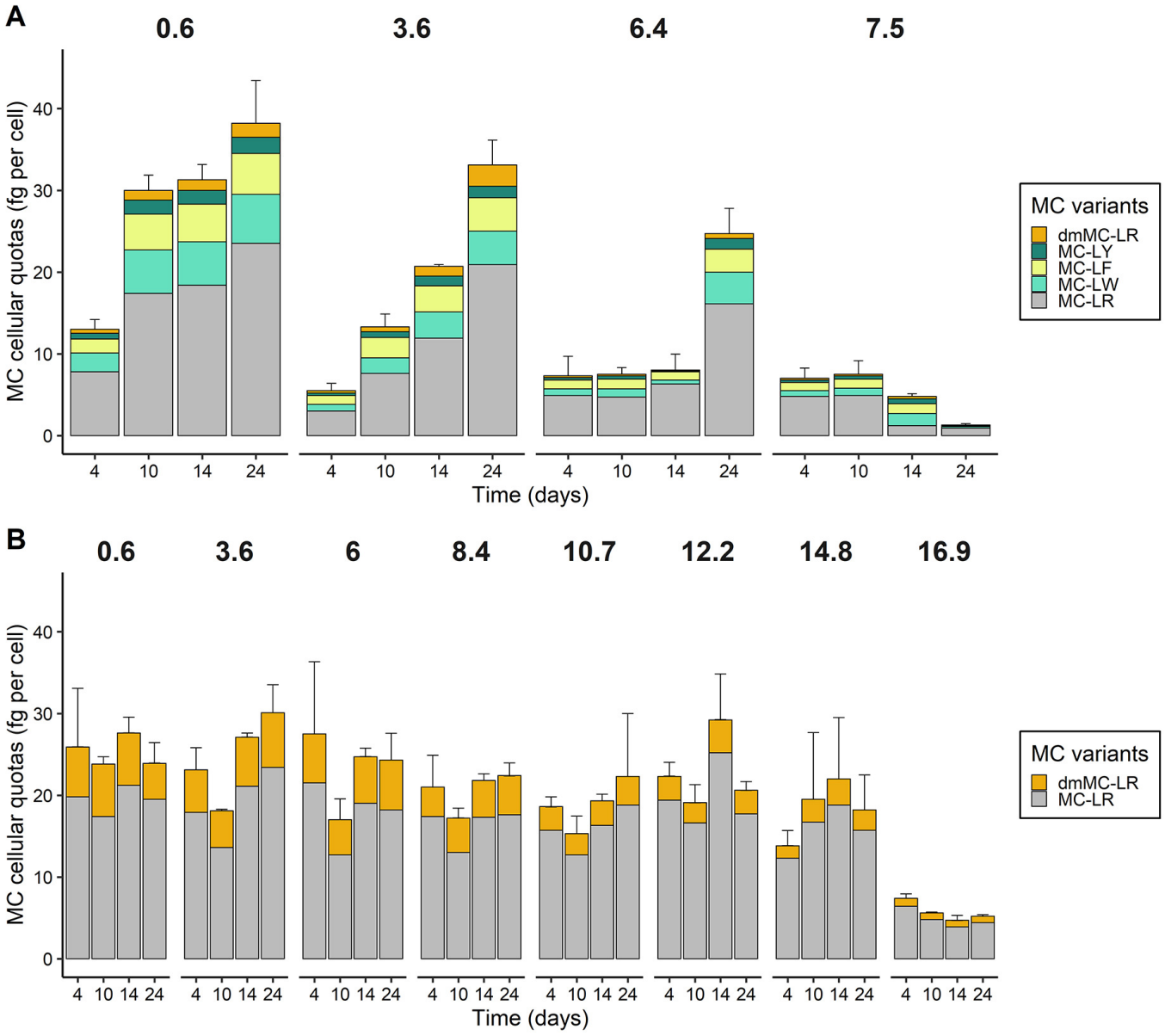

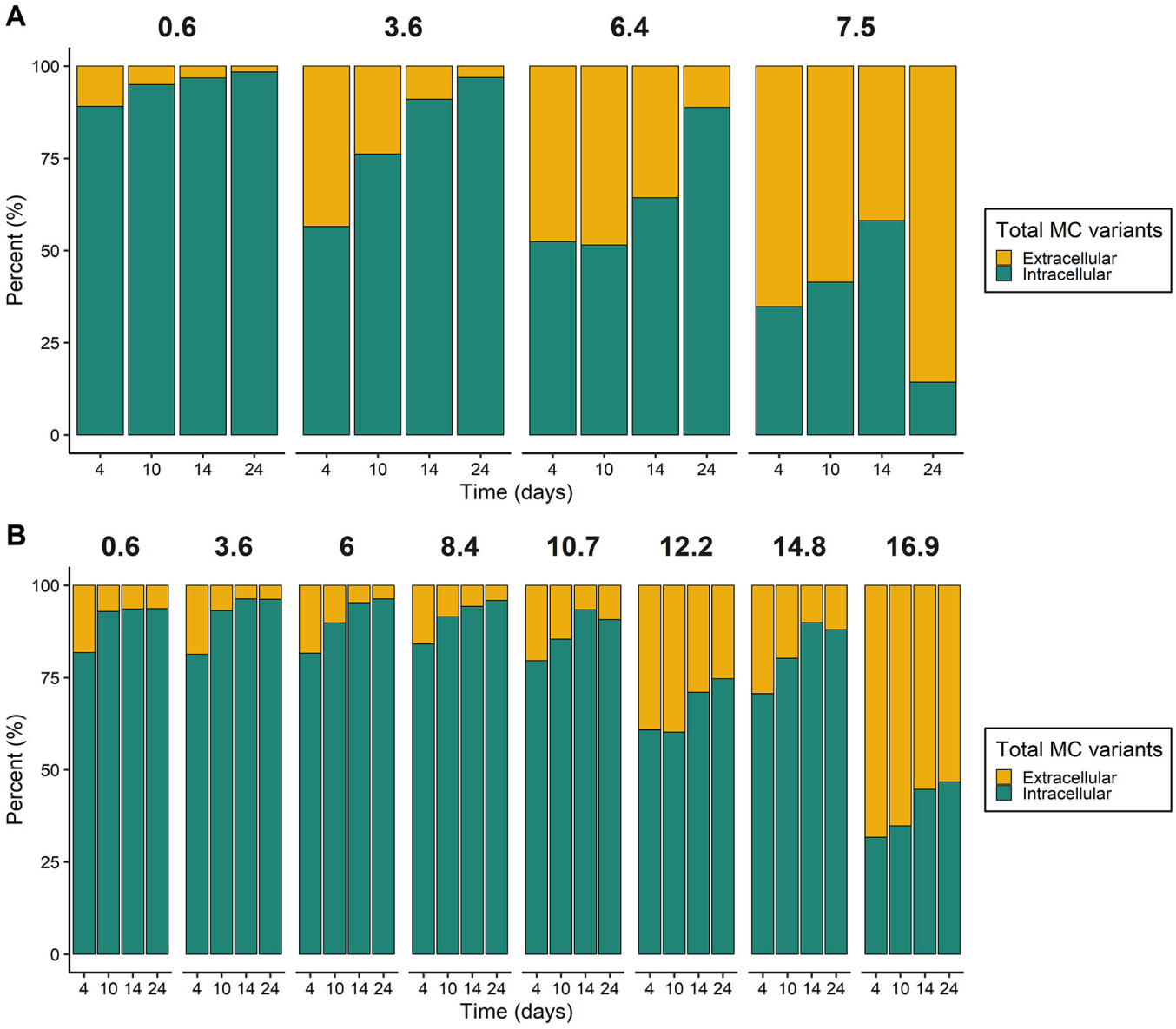

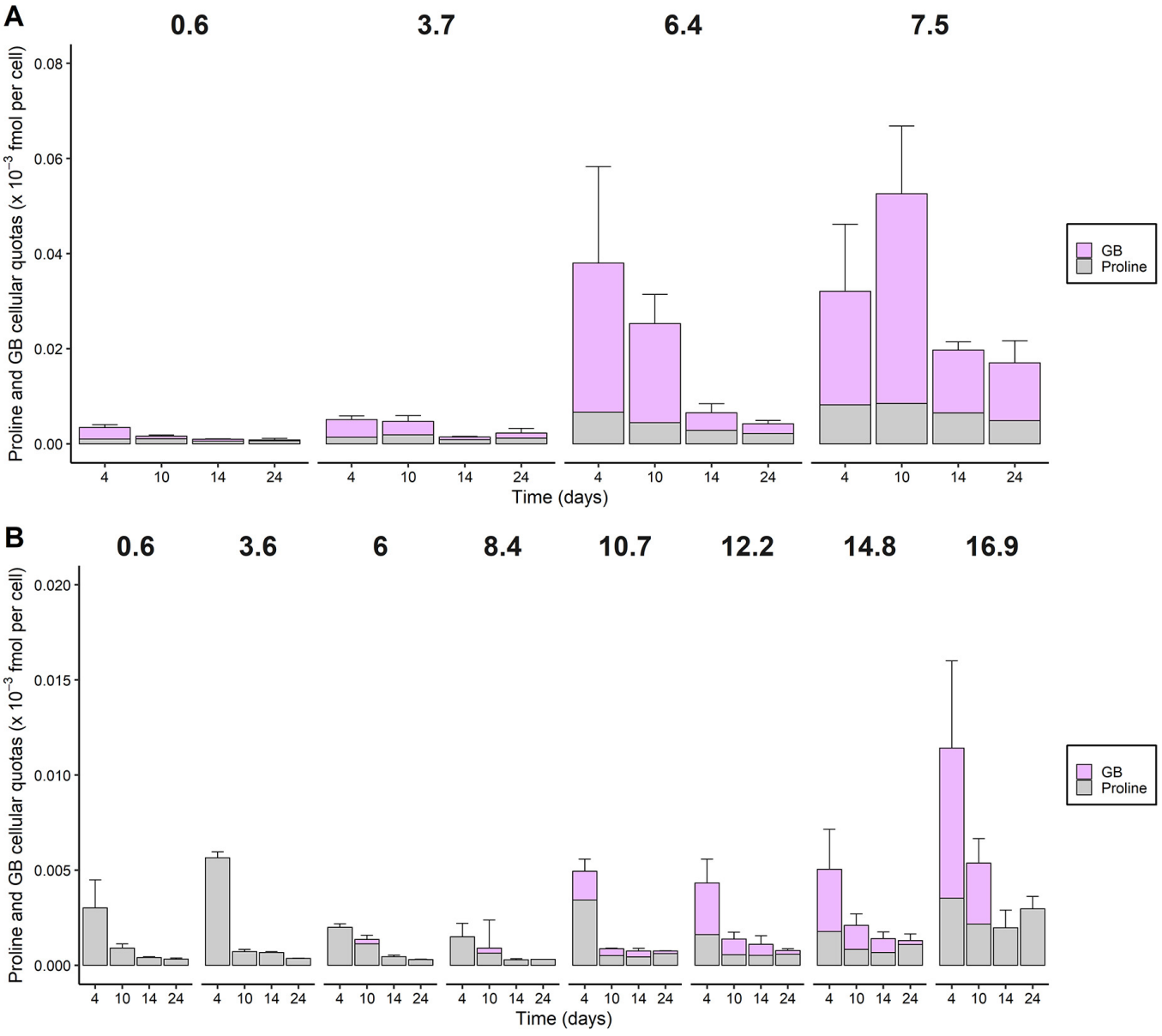

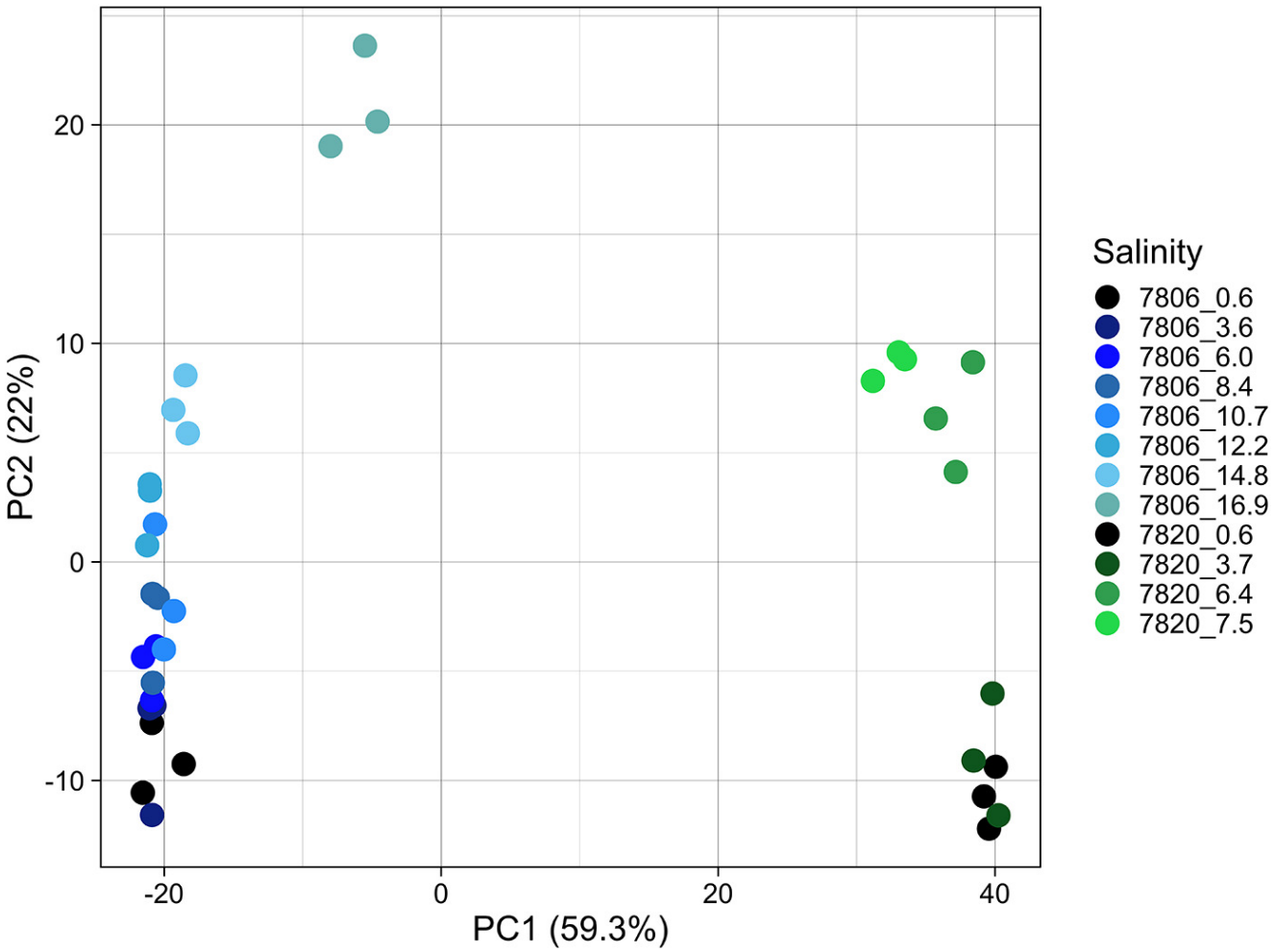

A

VIP number	VIP score	*m/z*	Retention time (s)	ID
1	2.1	365.1051	47	Trehalose (Level 1)
2	1.8	226.9520	36	NA
7	1.5	223.9896	34	NA
10	1.3	110.0089	34	NA
11	1.2	803.5639	634	MGDG (36:3) (Level 2)
12	1.2	631.1424	466	NA
13	1.2	927.6624	318	NA
3	1.6	935.5883	673	NA
4	1.5	903.5627	682	NA
5	1.5	981.5411	356	dmMC-LR (Level 2)
6	1.5	889.5833	716	NA
8	1.4	881.5781	667	NA
9	1.4	955.5447	566	NA
14	1.2	535.2874	446	NA

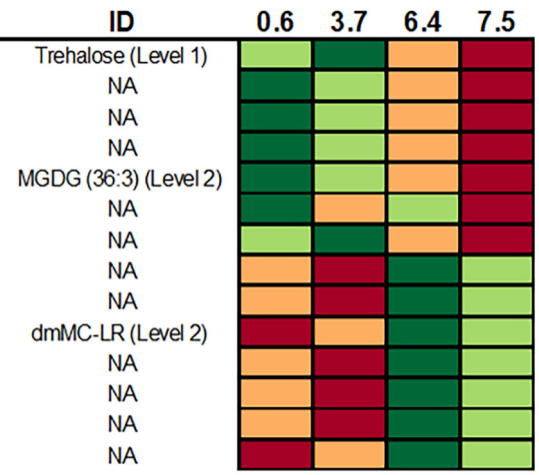

B

VIP score	*m/z*	Retention time (s)	ID
1.7	226.95	36	NA
1.7	223.99	34	NA
1.5	705.58	732	NA
1.5	110.01	34	NA
1.4	365.11	47	Sucrose (Level 1)
1.3	437.19	445	NA
1.2	803.56	634	MGDG (36:3) (Level 2)
1.2	775.53	626	MGDG (34:3) (Level 2)
1.1	777.55	631	MGDG (34:2) (Level 2)
1.2	677.37	455	NA
1.7	607.29	597	NA
1.7	535.29	446	NA
1.6	537.30	462	NA
1.6	889.58	716	NA
1.5	881.58	667	NA
1.5	943.55	367	Cyanopeptoline C (Level 2)
1.4	981.54	356	dmMC-LR (Level 2)
1.4	955.54	566	NA
1.2	519.24	340	NA
1.0	519.24	444	NA